



# Fabrication and properties of $\text{Si}_3\text{N}_4$ bioscaffolds with orderly–interconnected big pore channels and well–distributed small pores

Lijie Ma, Yuehai Song, Xiangming Li\*, Rui Li, Zhichao Shang, Yixuan Wang

School of Environment and Materials Engineering, Yantai University, Yantai Shandong 264005, PR China

## ARTICLE INFO

### Keywords:

$\text{Si}_3\text{N}_4$   
Bioscaffold  
Inverse replication  
3–D printing  
Vacuum suction filtration

## ABSTRACT

This paper focuses on investigating the technical potential for fabricating porous ceramic bioscaffolds for the repair of osseous defects from trauma or disease by inverse replication of three–dimensional (3–D) printed polymer template.  $\text{Si}_3\text{N}_4$  ceramics with pore structure comprising orderly–interconnected big pore channels and well–distributed small pores are successfully fabricated by a technique combining 3–D printing, vacuum suction filtration and oxidation sintering. The  $\text{Si}_3\text{N}_4$  ceramics fabricated from the  $\text{Si}_3\text{N}_4$  powder with addition of 10 wt% talcum by sintering at 1250 °C for 2 h have little deformation, uniform microstructure, low linear shrinkage of 4.1%, high open porosity of 58.2%, relatively high compression strength of 6.4 MPa, orderly–interconnected big pore channels and well–distributed small pores, which are promising bioscaffold in the field of bone tissue engineering.

## 1. Introduction

In the past two decades, bioscaffolds, which are used to fill in a bone cavity formed by trauma or disease and serve as a template for initial cell attachment, subsequent tissue formation and bone regeneration, have attracted much attention in the field of bone tissue engineering [1,2]. Generally, the bioscaffolds should have a bimodal pore structure comprising orderly–interconnected big pores with diameter larger than 100  $\mu\text{m}$  [3] and well–distributed small pores covering the diameter range of 2–5  $\mu\text{m}$  [4–6]. The orderly–interconnected big pores act as channels for the transport of body fluids, vessels and cells such as osteoclasts and osteoblasts, and the well–distributed small pores facilitate the attachment of cells and the excretion of metabolic waste [7,8].

$\text{Si}_3\text{N}_4$  ceramics with a high porosity of channels, well–controlled pore diameter distribution and tailored microstructure have generated great interest for their potential use in the applications of separation membranes, catalyst supports, gas filters, etc. [9,10]. Besides, porous  $\text{Si}_3\text{N}_4$  ceramics are promising bone substitute materials due to their good biocompatibility [11–14], and various techniques have been developed to fabricate porous  $\text{Si}_3\text{N}_4$  ceramics with well–distributed small pores [15–21]. As to an efficient bioscaffold, besides the well–distributed small pores, a sufficient quantity of big pores with pore diameter larger than 100  $\mu\text{m}$  is essential for enabling the invasion of cells [3] and increasing the number of cells for attachment [22]. More importantly, the big pores must connect well with each other for circulating the body fluids that transport osteogenic cells and nutrients

[23]. Obviously, the pore structure of the conventional porous  $\text{Si}_3\text{N}_4$  ceramics does not satisfy the criteria for an efficient bioscaffold.

So far, conventional ceramic foaming methods and pore–forming agent methods have been attempted to fabricate bioscaffolds [24–28]. However, these methods provide limited control over the pore structure of the bioscaffolds. Bioscaffolds with ordered pore structure were reported could be fabricated by inverse replication of assembled particles, and a  $\beta$ –tricalcium phosphate ceramic with an ordered arrangement of uniform big pores, high porosity and good pore interconnectivity was fabricated by ceramic slip casting using a particle–assembled template [8]. 3–D printing is a new and unique technique that prints complex structure and has demonstrated the capability of fabricating materials, including ceramics, metals, and polymers [18,29–34]. Several studies have investigated the application of 3–D printing for the fabrication of bioscaffolds for tissue engineering [35], and the feasibility of using 3–D printing to build bioscaffolds has been demonstrated by fabricating porous ceramic bioscaffolds with fully interconnected channel network from modified hydroxyapatite [36].

From the research mentioned above, it should be a feasible and controlled way to fabricate bioscaffolds with ordered pore structure by inverse replication of a polymer template with spatial lattice structure printed out by 3–D printer. The aim of this paper is to investigate the technical potential for fabricating porous  $\text{Si}_3\text{N}_4$  bioscaffolds with designed inner channels for bone tissue engineering by inverse replication of 3–D printed polymer template.  $\text{Si}_3\text{N}_4$  ceramics with a bimodal pore structure comprising orderly–interconnected big pore channels and

\* Corresponding author.

E-mail addresses: [li\\_xiangming@yahoo.com](mailto:li_xiangming@yahoo.com) (X. Li), [shangzhichao1996@163.com](mailto:shangzhichao1996@163.com) (Z. Shang), [wangyixuan970926@163.com](mailto:wangyixuan970926@163.com) (Y. Wang).

well-distributed small pores are fabricated by a technique combining 3-D printing, vacuum suction filtration and oxidation sintering.

In addition, to minimize the cost of  $\text{Si}_3\text{N}_4$  ceramics, the choice of sintering additive with reasonable costs as well as decreasing the sintering temperature are required. Talcum is considered as a low temperature and low cost sintering additive which was widely used as a flux to decrease the sintering temperature and improve the mechanical properties of ceramics [37,38]. Recently, porous  $\text{Si}_3\text{N}_4$  ceramics with uniform microstructure, good mechanical properties and high porosity were fabricated by using talcum and clay as sintering additives [39]. In this work, talcum is used as the sintering additive for  $\text{Si}_3\text{N}_4$  ceramics, and the effect of the talcum content on the shrinkage, porosity, composition, compression strength and microstructure of the  $\text{Si}_3\text{N}_4$  ceramics is discussed in detail.

## 2. Experimental procedure

### 2.1. Fabrication techniques

The templates with different spatial lattice structure were designed by using Unigraphics NX Software (Siemens PLM Software, Germany), and then sliced by Creaality 3D Software (Shenzhen Creaality 3D Technology Co. Ltd, China) to generate the printing matrix of each layer at every z-level. Fig. 1(a) shows one layer sliced from the template used in this work. The spatial lattice structure is formed by orderly arranging slender columns in X, Y and Z directions. The cross section of the columns is square with side length 0.4 mm, and the space among the columns in the three directions is 1.6 mm. Fig. 1(b) shows the polylactic acid templates with spatial lattice structure printed out by a 3-D printer (CR-10, Shenzhen Creaality 3D Technology Co. Ltd., China). In order to facilitate the following vacuum suction filtration process, all templates

are designed as square fluid directors consisting of a tube enclosed by four dense walls and openings at two ends of the tube, and the spatial lattice structure is located in the square tube.

$\text{Si}_3\text{N}_4$  powder ( $\alpha$  ratio > 90 wt%,  $\beta$  ratio < 10 wt%) was mixed with talcum powder ( $\text{Mg}_3[\text{Si}_4\text{O}_{10}](\text{OH})_2$ ) in ethanol, and then ball milled for 5 h into slurry. Fig. 2 schematic shows the fabrication process of the  $\text{Si}_3\text{N}_4$  ceramics with orderly-interconnected big pore channels and well-distributed small pores. Firstly, assembled the template, filter paper and template base with each other, and sealed the gaps between the template and base with vaseline. Secondly, started the vacuum pump connecting with the base and then added the slurry slowly into the template. In this step, the ethanol in the slurry adding in the template was sucked out gradually, and as a result the powder blend was retained and accumulated more and more in the template with the help of filter paper. As the template was fully filled with powder blend, stop adding slurry and kept the pressure in the chamber of the base at lower than 5 kPa for 2 h. Finally, the powder blend together with the template was taken out from the base and then sintered in a furnace at 1150–1300 °C for 2 h in air. During the sintering process, after removing the template because of oxidation, the  $\text{Si}_3\text{N}_4$  ceramics with orderly-interconnected big pore channels and well-distributed small pores were then obtained.

### 2.2. Characterization and tests

The microstructure was observed by scanning electron microscopy (SEM, JSM-7610F, JEOL, Japan). The phase analyses were conducted by X-ray diffraction (XRD, XRD-7000, Shimadzu, Japan). The shrinkage was estimated by measuring the dimensions of the template and the obtained samples after sintering. The open porosity was measured by Archimedes method. Five cylindrical samples of  $30 \times 15 \text{ mm}^2$  diameter were tested to obtain the average compression strength via uniaxial compression test (WDW-50, Hensgrand Instrument Co., Ltd. Jinan, China) with a loading speed of 0.5 mm/min. Before compression strength test, all samples were polished to get coplanar planes that were needed for uniaxial compression tests. For the convenience of the following discussion, the porous  $\text{Si}_3\text{N}_4$  ceramics fabricated from the powder blend with  $m$  wt% talcum at temperature of  $n$  °C is named as SN- $m$ - $n$  ( $m$  is 0, 5, 10 or 15,  $n$  is 1150, 1200, 1250 or 1300).

## 3. Results and discussion

Fig. 3 shows the liner shrinkage of porous  $\text{Si}_3\text{N}_4$  ceramics as a function of the talcum content in powder blend. The shrinkage of porous  $\text{Si}_3\text{N}_4$  ceramics shows equal values in X, Y and Z directions and increases with temperature rising. As the temperature rises from 1150 to 1300 °C, the shrinkage of SN-(0, 5, 10 and 15) increases respectively from 1.6%, 1.1%, 0.9% and 0.6% to 12.7%, 8.4%, 6.6% and 5.3%. During the sintering process at 1150–1300 °C, the amorphous  $\text{SiO}_2$  around  $\text{Si}_3\text{N}_4$  particles is in molten state [40,41], and the molten  $\text{SiO}_2$  draws the  $\text{Si}_3\text{N}_4$  particles closely with each other. The oxidation rate of  $\text{Si}_3\text{N}_4$  becomes higher with temperature rising from 1150 to 1300 °C, so the drawing effect of molten  $\text{SiO}_2$  enhances with the increase of oxidation-derived  $\text{SiO}_2$  and the shrinkage of porous  $\text{Si}_3\text{N}_4$  ceramics increases as a result. The addition of talcum could restrain effectively the shrinkage, deformation and crack of porous  $\text{Si}_3\text{N}_4$  ceramics, so the shrinkage of porous  $\text{Si}_3\text{N}_4$  ceramics decreases gradually with the increase of talcum in powder blend. As shown in Fig. 3, the shrinkage of SN-(1150, 1200, 1250 and 1300) decreases respectively from 1.6%, 4.2%, 7.3% and 12.7% to 0.6%, 1.5%, 3.2% and 5.3% with the increase of talcum in powder blend from 0 to 15 wt%.

As to the porous  $\text{Si}_3\text{N}_4$  ceramics fabricated from pure  $\text{Si}_3\text{N}_4$  powder, deformation and crack could hardly be found when the sintering temperature is 1150 °C, while them obviously when the sintering temperature is above 1200 °C. Fig. 4(a) shows the optic images of the as-obtained SN-0-1250 taken from different angles. As can be seen, the

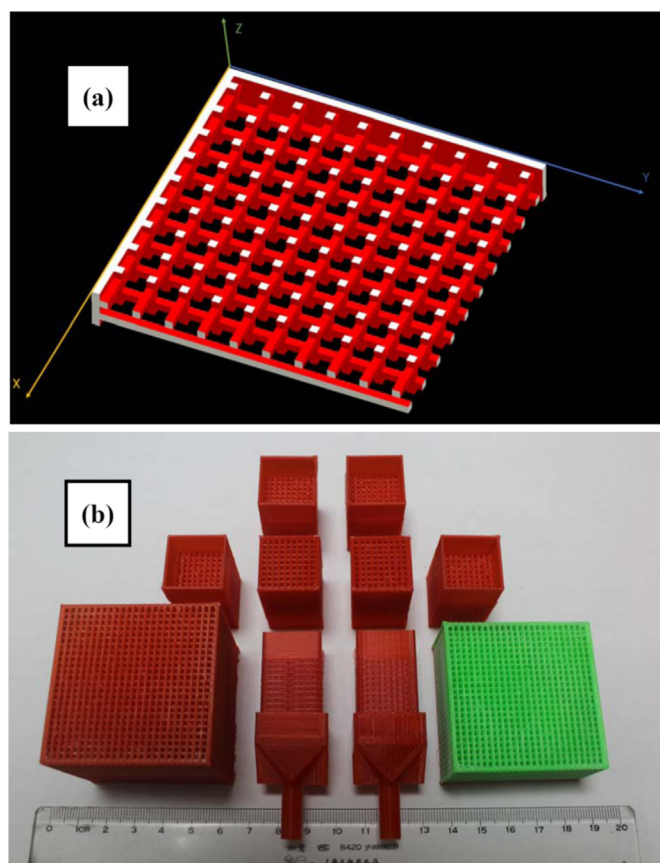


Fig. 1. (a) One layer sliced from the (b) polylactic acid templates with spatial lattice structure.

Download English Version:

<https://daneshyari.com/en/article/7887267>

Download Persian Version:

<https://daneshyari.com/article/7887267>

[Daneshyari.com](https://daneshyari.com)